Noname manuscript No.
(will be inserted by the editor)

Extended finite element method in computational fracture mechanics: a retrospective examination

N. Sukumar · J. E. Dolbow · N. Moës

Revised: December 1, 2015

Abstract In this paper, we provide a retrospective examination of the developments and applications of the extended finite element method (X-FEM) in computational fracture mechanics. Our main attention is placed on the modeling of cracks (strong discontinuities) for quasistatic crack growth simulations in isotropic linear elastic continua. We provide a historical perspective on the development of the method, and highlight the most important advances and best practices as they relate to the formulation and numerical implementation of the X-FEM for fracture problems. Existing challenges in the modeling and simulation of dynamic fracture, damage phenomena, and capturing the transition from continuum-to-discontinuum are also discussed.

Keywords elastic fracture, strong discontinuities, singularities, cracks, partition-of-unity enrichment, X-FEM

1 Introduction

The eXtended Finite Element Method (X-FEM) was introduced in Moës et al. (1999) as a new approach to represent fracture surfaces and to capture their evolution within a standard Galerkin-based method. Since its inception, the method has experienced dramatic growth and development. This is due to many factors, not the least of which is the potential of the X-FEM to circumvent long-standing issues in finite element mesh generation and adaptation for fracture problems. Moreover, even though there are many alternative numerical methods for fracture, none of them offer the combination of features that the X-FEM affords: extension to nonlinear problems, relative ease of implementation, robustness, efficiency and accuracy. In this paper, our intent is not to provide an exhaustive overview of the X-FEM; many such reviews are already available in the literature (Belytschko et al., 2009; Fries and Belytschko, 2010). Rather, we aim to provide an appraisal of the method for fracture problems: discussing the key advances, unifying and providing connections between previous contributions, and establishing best practices as they relate to the formulation and implementation of the method. We highlight the strengths and weaknesses of the method, and discuss missing gaps that can form the subject for future research.

The field of computational fracture mechanics is relatively mature, and many advances have been made with finite elements and boundary element methods. Nevertheless, fracture remains a challenging problem, and new methods continue to arise. With the standard finite element method, cracks are viewed as internal boundary surfaces that are explicitly meshed. The X-FEM is an advance in element technology — it allows for strong discontinuities (discrete cracks) to arbitrarily cut through elements. Prior to its introduction, there were many other approaches that addressed this challenge, among which,

N. Sukumar
Department of Civil and Environmental Engineering
University of California, Davis, CA 95616, U.S.A.
E-mail: nsukumar@ucdavis.edu
J. E. Dolbow
Department of Civil and Environmental Engineering
Duke University, Durham, NC 27708, U.S.A.
E-mail: jdolbow@duke.edu
N. Moës
GeM Institute, Ecole Centrale de Nantes, 44321 Nantes, France.
E-mail: nicolas.moes@ec-nantes.fr

enhanced assumed strain (Simo et al., 1993) and meshfree methods (Belytschko et al., 1996) are prominent.

Simo et al. (1993) considered embedded discontinuities from the viewpoint of the constitutive relationship. A local crack initiation criterion is posited within each element based on the loss of ellipticity (singularity of the acoustic tensor), and then the kinematics are enhanced in each element to accommodate this discontinuity. Due to the element-level nature of the formulation, this method leads to a nonconforming displacement approximation across element boundaries (compatibility of the strain field is weakly enforced). Furthermore, the initial approach did not ensure a continuous crack surface, which was subsequently corrected by incorporating linear interpolation between adjacent elements (Linder and Armero, 2007). For a discussion of various early finite element methods that embed discontinuities, we direct the reader to the work of Jirásek (2000).

The partition-of-unity finite element method (PUFEM) (Melenk and Babuška, 1996; Babuška and Melenk, 1997) permits local asymptotic crack solutions (enrichment functions) to be incorporated within a finite element (FE) setting. This notion of augmenting the standard FE approximation by known asymptotic solutions is not new (Fix et al., 1973; Strang and Fix, 1973; Benzley, 1974); however, in these prior studies, the additional functions are added globally to the finite element approximation. Moreover, these approaches are in stark contrast to the PUFEM, where the finite element basis functions are used to partition the enrichment function so that all basis functions are compactly-supported. The resulting stiffness matrix is symmetric and banded, and its sparsity is not significantly compromised. Another instance of the PUFEM is the generalized finite element method (GFEM), in which handbook solutions and eigenfunctions for corner singularities and crack problems in elasticity are selected as enrichment functions (Duarte et al., 2000; Strouboulis et al., 2001).

On using finite elements to form the partition-of-unity functions as introduced in the PUFEM, Belytschko and Black (1999) adopted a *local or minimal enrichment* perspective to enrich the finite element approximation with the asymptotic crack-tip basis functions (Fleming et al., 1997) to model two-dimensional cracks (crack interior and crack tips), which were represented by the union of piecewise linear segments. This required a series of mappings to describe such a crack. On using a discontinuous (generalized Heaviside) enrichment function, a much simpler approach to model the crack interior was realized by Moës et al. (1999), and this method was coined as the extended finite element method (X-FEM) (Daux et al., 2000). For modeling cracks, discontinuous enrichment is now also adopted in the GFEM (Simone et al., 2006; Duarte and Kim, 2008), and hence for fracture problems, the X-FEM and the GFEM are practically indistinguishable.

In the X-FEM, crack discontinuities are incorporated via the kinematics: the displacement field is enriched with discontinuous and crack-tip asymptotic functions. The X-FEM permits simple meshes to be used that need not conform to the crack geometry, thereby avoiding the need to remesh for crack propagation simulations. For crack modeling and crack growth problems in isotropic linear elastic fracture mechanics, the advantages of the X-FEM over C^0 Lagrange finite elements have been well-established. In this paper, our main emphasis is on the modeling of elastic fracture with the X-FEM. In Sect. 8, we also share our perspectives on using the X-FEM and other emerging methods for the modeling of dynamic fracture, damage and other challenging problems in inelastic fracture mechanics.

2 Formulation

Consider a homogeneous linear elastic body that occupies the domain $\Omega \subset \mathbb{R}^d$ $(d = 2, 3)$ with an internal traction-free crack. The boundary $\Gamma = \Gamma_u \cup \Gamma_t \cup \Gamma_c$ with $\Gamma_u \cap \Gamma_t = \emptyset$ (see Fig. 1). Displacement boundary conditions are prescribed on Γ_u, and tractions are imposed on Γ_t. The crack domain is Γ_c, and we denote the crack front (crack tip in $\mathbb{R}^2$) by Λ_c. The governing equations for elastostatics in the absence of body forces are:

$$\boldsymbol{\nabla} \cdot \boldsymbol{\sigma} = \mathbf{0} \text{ in } \Omega, \tag{1a}$$

$$\boldsymbol{\sigma} = \boldsymbol{C} : \boldsymbol{\varepsilon}, \tag{1b}$$

$$\boldsymbol{\varepsilon} = \boldsymbol{\nabla}_s \boldsymbol{u}, \tag{1c}$$

where $\boldsymbol{\sigma}$ is the Cauchy stress tensor, $\boldsymbol{u}$ is the displacement field, $\boldsymbol{\varepsilon}$ is the small-strain tensor, $\boldsymbol{\nabla}_s$ is the symmetric gradient operator, and $\boldsymbol{C}$ is the material moduli tensor for a homogeneous linear elastic isotropic material. The essential and natural boundary conditions are:

$$\boldsymbol{u} = \bar{\boldsymbol{u}} \text{ on } \Gamma_u, \tag{2a}$$

$$\boldsymbol{\sigma} \cdot \boldsymbol{n} = \bar{\boldsymbol{t}} \text{ on } \Gamma_t, \tag{2b}$$

$$\boldsymbol{\sigma} \cdot \boldsymbol{n} = \mathbf{0} \text{ on } \Gamma_c, \tag{2c}$$

where $\boldsymbol{n}$ is the unit outward normal on a boundary, and $\bar{\boldsymbol{u}}$ and $\bar{\boldsymbol{t}}$ are the prescribed displacements and tractions on Γ_u and Γ_t, respectively.

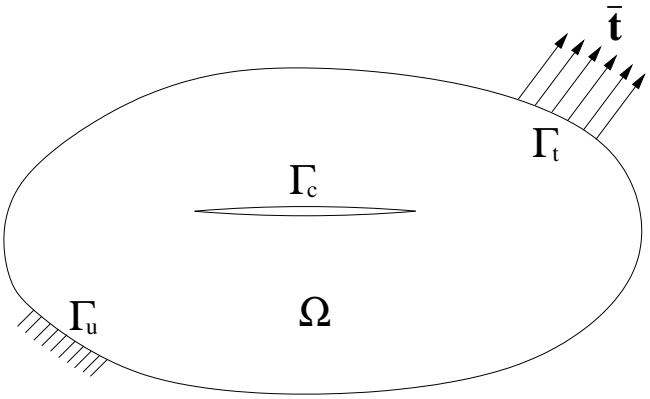

Fig. 1: Elastostatic boundary-value problem with an embedded traction-free crack.

The weak form of the boundary-value problem posed in (1) and (2) is: find $\boldsymbol{u} \in \mathcal{U}$ such that

$$a(\boldsymbol{u}, \delta\boldsymbol{u}) = \ell(\delta\boldsymbol{u}) \quad \forall \delta\boldsymbol{u} \in \mathcal{U}_0, \tag{3a}$$

$$a(\boldsymbol{u}, \delta\boldsymbol{u}) := \int_\Omega \boldsymbol{\sigma} : \delta\boldsymbol{\varepsilon}\, d\boldsymbol{x}, \quad \ell(\delta\boldsymbol{u}) := \int_{\Gamma_t} \bar{\boldsymbol{t}} \cdot \delta\boldsymbol{u}\, dS, \tag{3b}$$

where $\mathcal{U}$ and $\mathcal{U}_0$ are the trial space for the displacement field and the test space (virtual displacements), respectively. The trial and test spaces admit functions that are discontinuous across Γ_c.

3 Displacement approximation

To discretize the weak form in (3), we require trial and test approximations for the displacement field. Consider a finite element mesh that discretizes the two-dimensional domain (without considering Γ_c) shown in Fig. 1. The embedded crack shown in Fig. 2 has two crack tips. Let the number of nodes of a given finite element be nen, and the index set $\mathbb{I} := \{1, 2, \ldots, nen\}$. Now, the two-dimensional extended finite element displacement approximation in an element takes the form (Moës et al., 1999):

$$\boldsymbol{u}_e^h(\boldsymbol{x}) = \underbrace{\sum_{i\in\mathbb{I}} N_i(\boldsymbol{x})\boldsymbol{u}_i}_{\text{standard FE}} + \underbrace{\sum_{j\in\mathbb{J}\subseteq\mathbb{I}} N_j(\boldsymbol{x})\varphi(\boldsymbol{x})\boldsymbol{a}_j}_{\text{discontinuous contribution}} + \underbrace{\sum_{t=1}^{2}\sum_{k\in\mathbb{K}_t\subseteq\mathbb{I}} N_k(\boldsymbol{x})\sum_{\alpha=1}^{4} F_{\alpha t}(\boldsymbol{x})\boldsymbol{b}_{k\alpha t}}_{\text{crack-tip contribution}}, \tag{4a}$$

with

$$\boldsymbol{F}_{\alpha t}(\boldsymbol{x}) = \sqrt{r}\left\{\sin\frac{\theta}{2}, \cos\frac{\theta}{2}, \sin\frac{\theta}{2}\sin\theta, \cos\frac{\theta}{2}\sin\theta\right\}, \tag{4b}$$

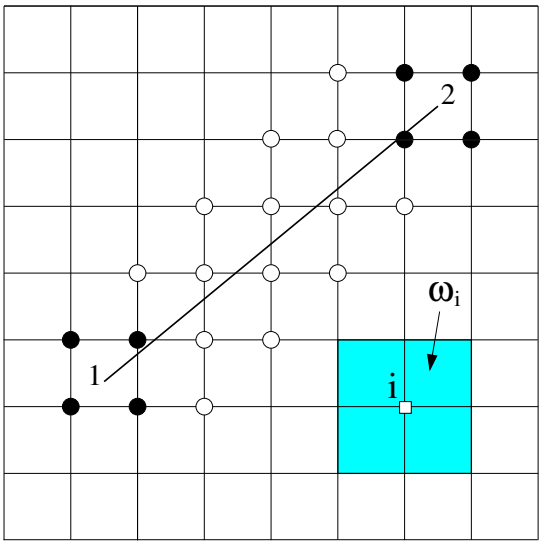

Fig. 2: Enriched nodes for an embedded crack. The crack-tips are labeled as 1 and 2. The nodes that are enriched with the discontinuous function are shown by open-circles, whereas those that are enriched with the asymptotic near-tip crack functions are shown by filled-circles. The shaded region is the support ω_i of the nodal finite element basis function for node i.

where $\mathbb{J}$ is the index set of nodes whose basis function support is cut by the interior of the crack Γ_c, and $\mathbb{K}_1$ and $\mathbb{K}_2$ are the index sets of nodes whose basis function support contains the crack-tips Λ_c^1 and Λ_c^2, respectively. In addition, $N_i(\boldsymbol{x})$ are the finite element shape functions, $\varphi(\boldsymbol{x})$ is a discontinuous (generalized Heaviside) function that is defined with respect to the crack, and $F_{\alpha t}(\boldsymbol{x})$ in (4b) are the crack-tip asymptotic functions defined with respect to a polar coordinate system (r, θ) with origin at the crack-tip t. If the crack-tip is located inside a finite element, then crack-tip enrichment is needed to represent the crack; enriching with the functions in (4b) also significantly improves the accuracy of the stress intensity factors in extended finite element computations. The unknown coefficients in (4a) corresponding to the standard FE, discontinuous, and near-tip basis functions are $\boldsymbol{u}_i$, $\boldsymbol{a}_j$, and $\boldsymbol{b}_{k\alpha t}$, respectively. The enriched nodes contained in $\mathbb{I}$, $\mathbb{J}$ and $\mathbb{K}_t$ $(t = 1, 2)$ are shown in Fig. 2.

Arguably the most successful and widely-implemented aspect of the approximation (4) is the generalized Heaviside enrichment — $\varphi(\boldsymbol{x}) := H(\boldsymbol{x})$, where given the orientation of the crack, $H(\boldsymbol{x})$ assumes a value $+1$ above the crack and a value -1 below it. This may be due to several factors. Whereas the near-tip enrichment functions are specifically designed for problems in linear elastic fracture mechanics, the Heaviside enrichment suffers no such

limitations. It has been applied in a wide range of contexts, including finite deformation problems and inelasticity. It is also the simplest aspect of the approximation to implement, as it only requires knowledge of which side of the discontinuity a material point resides.

Another component to the success of Heaviside enrichment concerns the work of Hansbo and Hansbo (2004). Consider an element that is separated into two distinct material regions by a crack geometry. Instead of using enrichment to capture the discontinuity, Hansbo and Hansbo (2004) proposed an approach that creates two *partial* elements, one for each side of the crack. Earlier, Jirásek and Belytschko (2002) had illustrated the same idea for a discontinuity in one dimension. For each partial element, newly defined shape functions are associated with all the nodes of the element. Furthermore, for each component of the displacement approximation, double the number of shape functions contribute in the element. The standard nodal Lagrange finite element shape function is decomposed into the sum of two discontinuous functions, which serve as the two new nodal shape functions — each is nonzero on one of the partial elements and is identically zero on the other. In a subsequent work, Areias and Belytschko (2006) illustrated how the kinematics that are enabled by this approach are in fact identical to what can be achieved via Heaviside enrichment. Implementations of both approaches can be found in modern production codes. The particular choice largely depends on the structure of the code and the ease of implementation (see Sect. 3.4). We point out that the approach of Hansbo and Hansbo (2004) is sometimes referred to as the *phantom-node* method (Song et al., 2006).

Over the past decade, several other modifications to the approximation (4) and enrichment functions have been proposed. Perhaps the most important is the concept of *geometric* enrichment (Laborde et al., 2005; Béchet et al., 2005). For the initially proposed extended finite element approximation in (4a), the set $\mathbb{K}_t$ of nodes with near-tip enrichment was limited to those nodes whose basis function support contained a crack-tip. This is often referred to as *topological* enrichment. With topological enrichment, the square root crack-tip singularity limits the convergence rate, and $\mathcal{O}(h^{1/2})$ decay in the energy seminorm of the error is realized, which matches the convergence rate that is obtained using quarter-point finite elements. With geometric enrichment, the enriched nodal set is expanded to all nodes within a specified distance from a crack-tip. This permits near-tip enrichment to be active over the entire region where the asymptotic fields dominate the solution, which translates to significant improvements in accuracy. Moreover, this radius of influence is taken to be independent of the mesh, such that the cardinality of $\mathbb{K}_t$ increases with refinement. Even though the stress field is singular, geometric enrichment allows the method to yield the same rates of convergence that are available for smooth problems (Strang and Fix, 1973; Nicaise et al., 2011). The drawback to this approach is that it increases the system size and impacts conditioning, but the latter can be addressed with suitable preconditioners (see Sect. 5).

We also discuss blending elements (elements that have partially enriched nodes) (Chessa et al., 2003) and the use of shifted enrichment functions. The former is especially pertinent for material interface problems, in which use of the distance function as the enrichment led to suboptimal rates of convergence (Sukumar et al., 2001). For this choice of the enrichment function, the extended finite element approximation cannot pass the patch test (affine field on either side of a rectilinear interface) for a bimaterial interface problem. A subsequent advance — use of the ridge enrichment function (Moës et al., 2003) for material interfaces — yielded optimal convergence rates without the presence of blending elements. However, it is noteworthy to point out that the presence of blending elements does not compromise the convergence rates for crack problems with near-tip enrichment, provided that geometric enrichment is adopted (Béchet et al., 2005; Fries and Belytschko, 2010; Nicaise et al., 2011).

The use of a shifted enrichment function (Zi and Belytschko, 2003) was introduced in part to facilitate plotting and to avoid the presence of blending elements when certain enrichment functions are used. A shifted enrichment simply adjusts the enrichment functions so that they vanish at the nodes; fundamentally, it does not change the approximation. A shifted enrichment ensures that the extended FE approximant becomes a nodal interpolant; however, this alone does not provide a means to impose Dirichlet boundary conditions. Furthermore, if a node with coordinate $\boldsymbol{x}_i$ lies on a crack, then $H(\boldsymbol{x}_i)$ is multi-valued and then a consistent choice for $H(\boldsymbol{x}_i)$ needs to be made. We also note that while this shifting might appear to facilitate plotting, such an approach effectively hides the singularity and discontinuity, both of which are vital to accurately displaying field quantities near the crack for fracture problems.

As an aid to understanding the basis functions in the different approaches, we present a one-dimensional example. Consider a one-dimensional domain that is discretized by linear finite elements, which must permit a discontinuity in the field variable at $x = \xi$, where $\xi \in \Omega_e = (x_1, x_2)$. Let the node at $x = x_1$ be labeled as 1 and the node at $x = x_2$ be labeled as 2. We consider all the basis functions that are associated with nodes 1

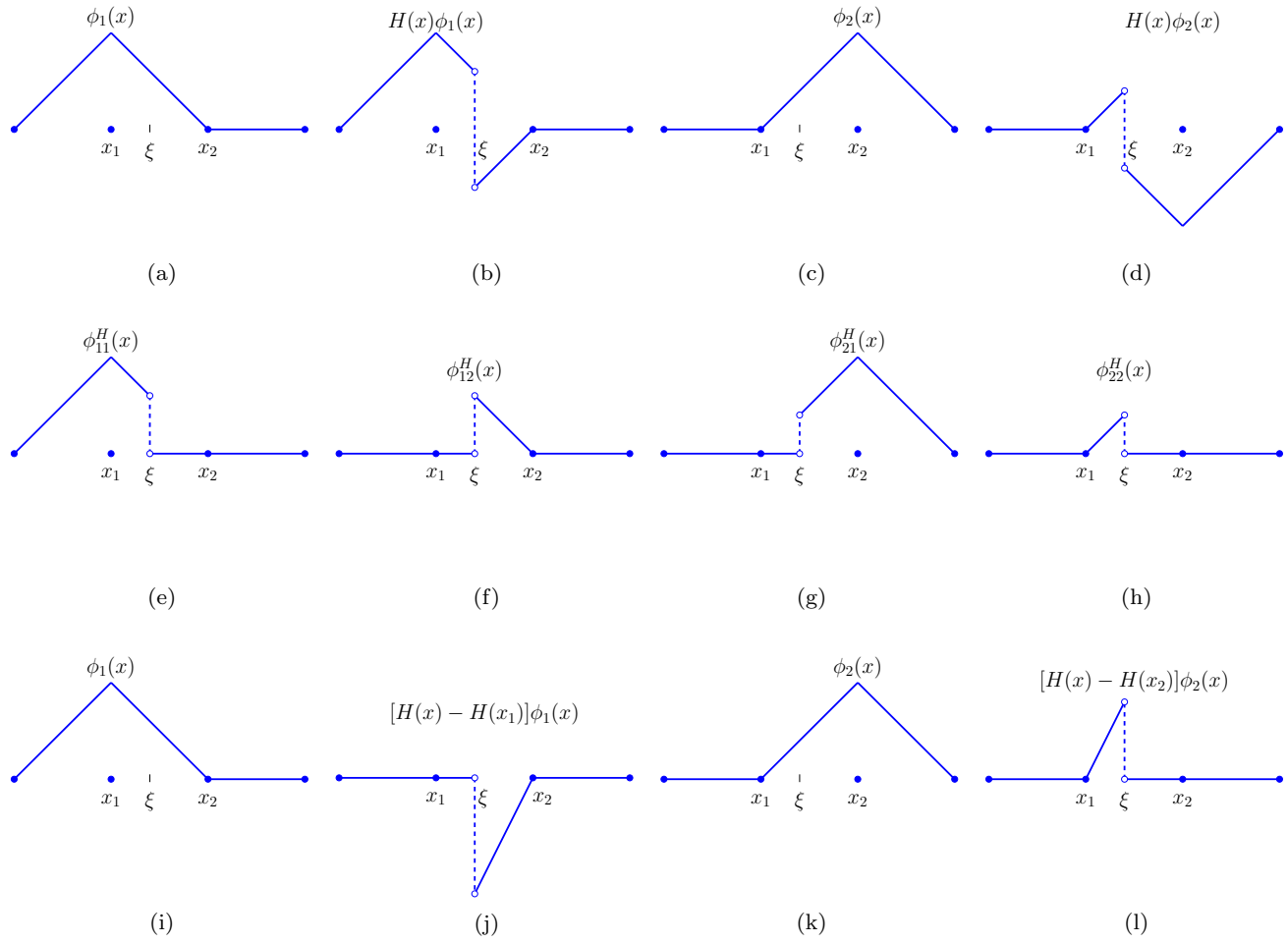

Fig. 3: Basis functions for a discontinuity in one dimension. (a)–(d) X-FEM with generalized Heaviside enrichment; (e)–(h) Approach of Hansbo and Hansbo (2004); and (i)–(l) Shifted Heaviside enrichment.

and 2; the support of these basis functions intersect Ω_e. The basis functions in the X-FEM, those obtained using the approach of Hansbo and Hansbo (2004), and the basis functions using shifted Heaviside enrichment are shown in Fig. 3. Referring to Fig. 3, we can write down the extended finite element basis functions in terms of those in Hansbo and Hansbo (2004) as:

$$\phi_1(x) = \phi^H_{11}(x) + \phi^H_{12}(x),\ H(x)\phi_1(x) = \phi^H_{11}(x) - \phi^H_{12}(x),$$
$$\phi_2(x) = \phi^H_{21}(x) + \phi^H_{22}(x),\ H(x)\phi_2(x) = \phi^H_{21}(x) - \phi^H_{22}(x),$$

which shows that the two sets of basis functions span the same discrete space.

3.1 Branched and intersecting cracks

The geometry of a crack or system of cracks can of course be much more complex than that shown in Figure 2. For example, a rapidly propagating crack can undergo a bifurcation and branch dynamically, splitting into two new crack fronts. More generally, multiple crack fronts can exist at one point in time and subsequently interact, potentially merging. Although multiple crack tips in close proximity do present their own set of challenges for asymptotic enrichment, most of the research effort has been focused on strategies to handle the *interior* of the crack network. In other words, the emphasis has once again been on enhancing the approximation such that the kinematics associated with a network of cracks (intersecting and/or branched) are properly represented.

Early work along these lines by Daux et al. (2000) considered cracks with multiple branches and the need for additional types of enrichment functions for the interior. Consider, for example, the case of two independent cracks that cross each other. At their crossing point, or junction, a naive approach is to simply enrich each crack with its own Heaviside function. Through comparison with an analogous system that is explicitly meshed, it is

shown in Daux et al. (2000) that these two enrichment functions are not sufficient to represent all the kinematics that ensue due to two cracks crossing. There are additional opening modes that need to be captured. This was resolved by identifying a *main* crack and any associated branches, and by adding junction enrichment functions that exhibited discontinuities across both the main crack and their respective branches. An improvement for junction enrichment that applies in two and three dimensions was proposed by Simone et al. (2006).

Alternative strategies have also been developed by the computer graphics community. The virtual node algorithm developed by Molino et al. (2004) can be viewed as an extension of the Hansbo-Hansbo approximation for multiple cracks. Each partial element is viewed as consisting of *physical* and *virtual* nodes. In this approach, virtual nodes are created based on the number of unique partitions (by crack geometry) formed in the region defined by the support of the first-order nodal basis functions (nodal one-rings). New partial elements are then created based on the topology and connectivity of the physical and virtual nodes. This approach naturally handles the case when a crack branches within an element, and it generalizes to three-dimensional problems. It bears emphasis that the resulting kinematics are identical to what can be obtained through Heaviside and junction enrichment.

More recently, Richardson et al. (2011) proposed a method for geometrically elaborate cracks. In contrast to the nodal-based approach of Molino et al. (2004), this is an element-based approach to creating new partial elements. The first step is to identify all distinct material regions in each element as dictated by the fracture geometry. In an intermediate step, partial elements are generated for each of the material regions in each of these elements. The final step reconnects these partial elements and collapses degrees of freedom based on common material regions at element edges (or faces in three dimensions). As pointed out by Richardson et al. (2011), in some cases this approach results in element kinematics that are distinct from what can be achieved via traditional enrichment algorithms.

3.2 Adaptivity

The basic approximation (4a) of the X-FEM is constructed using both standard finite element and enriched basis functions. Both these classes of basis functions rely on an underlying finite element mesh. While such an FE mesh can be constructed independent of the crack geometry, it nonetheless impacts the accuracy of the fracture simulation. In general, the accuracy of a given extended FE simulation is governed by the structure of the FE mesh and the form of the near-tip enrichment (geometric or topological). In order to ensure a desired level of accuracy, the background mesh will usually need to be adaptively refined or some form of r-adaptivity will be required to construct a suitable mesh. However, irrespective of the choice made, it is important to emphasize that the process of adaptivity is greatly simplified since the mesh need not conform to the crack geometry. It is much simpler to locally refine a mesh in a region to some specific level of resolution than it is to construct a mesh that conforms to a crack, and this is especially so in three dimensions.

Adaptivity with the X-FEM can be driven by several considerations. In particular, we focus on the representation of the crack geometry, the accuracy of the approximate displacement field, and the extraction of stress intensity factors. The first two are intimately related. On the one hand, the geometry of a crack or fracture network can be captured by adapting the integration cells within elements that contain cracks. When Heaviside enrichment is then added to the standard FE approximation, the kinematics of the crack geometry can be captured by the displacement approximation, albeit with some caveats. For example, a single Heaviside function cannot capture multiple cracks that pass through a single element, and perhaps more importantly, it cannot capture cracks that terminate inside elements. The use of Heaviside enrichment alone implies that crack tips terminate on element edges, which is limiting for many fracture applications.

Near-tip enrichment not only allows a more precise representation of the crack-tip geometry, it also improves the accuracy of the displacement approximation by introducing singular fields. But here too, there are limits to the basic extended finite element approximation (4a) as discussed in Bellec and Dolbow (2003). For cracks that are sufficiently small relative to the mesh size, the near-tip enrichment functions cease to be appropriate. In these limiting cases, discontinuities in near-tip enrichment functions can extend too far, beyond the end of the crack on the other side. To some degree, accuracy can be recovered by modifying the near-tip enrichment to account for both tips.

Regarding stress intensity factors, if several crack tips or fronts lie within the same element, it is difficult to separate contributions from each of them using domain and interaction integrals. It is thus reasonable to adaptively refine meshes so that several elements separate distinct tips and fronts whenever possible. Such heuristics are less than satisfactory. More generally, the appropriate level

of mesh refinement needs to be analyzed through *a posteriori* error estimation techniques. Such error estimation tools for the X-FEM have been designed, for example, see Rodenas et al. (2008) and Duflot and Bordas (2008).

An interesting two-scale approach has been proposed by Duarte and Kim (2008) for static cracks and extended to propagating cracks in Pereira et al. (2011). The idea is to use a fixed global mesh with finer, nested meshes to obtain accurate fields near crack fronts. The macro problem on the global mesh uses enrichment functions that are computed on the fine local grids using boundary conditions of the global problem (at the previous step). This decomposition between the two scales not only reduces the computational time but also allows the global mesh to remain fixed.

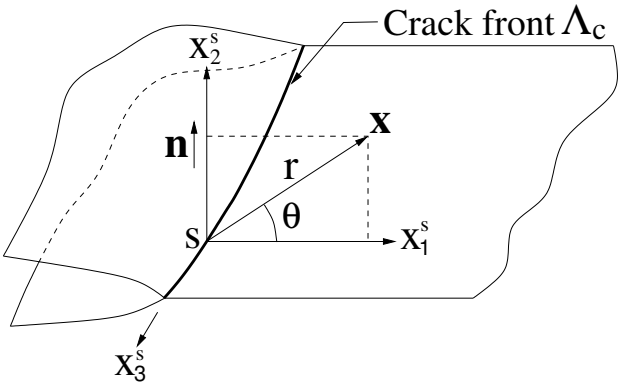

Fig. 4: Local coordinate system for crack front enrichment.

3.3 Extension to three dimensions

The displacement approximation (4) directly extends to three dimensions. The crack geometry in three dimensions is described by a surface (crack interior) and a boundary curve (crack front). As enrichment functions, the generalized Heaviside function is used for the crack interior and the two-dimensional (plane-strain) asymptotic functions given in (4b) are used for the crack front. The definitions for the sets of enriched nodes are identical to the two-dimensional case. For example, all nodes whose basis function support contains the crack front are enriched with the near-tip functions. In three dimensions, a local crack-tip coordinate system (r, θ) is attached to each point s on the crack front (see Fig. 4). For a given integration point $\boldsymbol{x} \in \Omega$, the point s on the crack front is needed to determine the local coordinate system to compute the enrichment functions as well as in post-processing to extract the stress intensity factors using the domain form of the contour interaction integrals. In finite element analysis, a nonlinear Newton iterative scheme is needed to compute the shortest distance, which is then used to set up the local coordinate system at s (Gosz and Moran, 2002). An implicit representation of the crack geometry using level sets greatly simplifies these computations in the X-FEM (see Sect. 6).

While it is common to use the four functions (4b) for both two and three-dimensional problems, it bears emphasis that they are only asymptotic under plane-strain conditions. Many fracture problems in three dimensions have cracks that intersect a free surface, where the nature of the singularity changes. Theoretical analysis due to Benthem (1977) reveals that the strength of the singular fields near a free surface depends on the Poisson's ratio ν. For $\nu = 0$, a $r^{-1/2}$ singularity in the near-tip stress field exists, as one might expect. However, for $\nu > 0$, the strength of the singularity is generally less than $1/2$. This variation in the singularity near the free surface is neglected in most studies that use the X-FEM. In very recent work, González-Albuixech et al. (2015) modify the enrichment functions to account for free-surface effects, which shows improvements in the accuracy of the extended finite element computations.

We also mention some alternatives to near-tip enrichment in three dimensions. Consider a standard eight-node trilinear brick element, which employs eight standard shape functions and 24 degrees of freedom to approximate a vector-valued displacement field. When near-tip enrichment is added in the form of (4b), an additional 12 degrees of freedom per enriched node are required. As such, an eight-noded element with all nodes enriched with near-tip functions employs 120 degrees of freedom (24 standard and 96 enriched).

One approach to reduce this relatively large number of degrees of freedom and still capture the asymptotic field is to employ *vectorial* enrichment. The use of vectorial enrichment for crack problems was first introduced in Duarte et al. (2000). With the standard near-tip enrichment, each of the four scalar enrichment functions (4b) are multiplied by vectorial degrees of freedom $\boldsymbol{b}_{k\alpha t}$. By contrast, vectorial enrichment uses three vector-valued enrichment functions that are each multiplied by scalar degrees of freedom. The result is that the number of additional degrees of freedom per enriched node is reduced from 12 to 3. Recent work by Chevaugeon et al. (2013) and Gupta et al. (2015) in two and three dimensions, respectively, demonstrate that when combined with the geometric enrichment strategy, use of vectorial enrichment provides the same level of accuracy at reduced computational cost.

3.4 Programming

The extended finite element approximation (4a) can be a challenge to incorporate into standard finite-element programs, depending on the structure of the basic code and its ability to manage degrees of freedom. Rather than a standard *element-centric* philosophy, the X-FEM adopts a *nodal-centric* viewpoint when building an enriched approximation. As indicated in Fig. 2, this gives rise to elements with variations in both number and type of degrees of freedom. The number of enriched nodes for an element can be zero, one, or all the nodes of the element. More generally, elements can have a mix of standard, near-tip, and Heaviside degrees of freedom.

Many finite-element programs assume that all elements within a block have the same number of degrees of freedom. Using mesh structures that respect this restriction helps to optimize memory and reduce latency for parallel calculations. When only Heaviside enrichment is used, such structures can easily be maintained by adopting the partial element approach of Hansbo and Hansbo (2004). With near-tip enrichment, one (very inefficient) approach is to construct a mesh of elements with all nodes enriched, and then to simply fix degrees of freedom to zero for those nodes with basis function supports that are far away from any crack tip.

Beyond these basic considerations, there are many technical aspects to consider to properly and efficiently handle the interaction between an arbitrary crack geometry and a background mesh. This includes the utilization of geometric predicates to deal with tolerances and recursive algorithms for constructing integration cells. For details into these issues, we refer the reader to discussions in Sukumar et al. (2000) and Sukumar and Prévost (2003). Importantly, the enrichment strategies of the X-FEM have been successfully incorporated into a wide range of commercial and research codes: for example, `Abaqus`, `LS-DYNA`, `Code_Aster` and `GetFem++` to name just a few.

4 Numerical computation of weak form integrals

On using trial and test functions of the form (4) in the weak form (3), we obtain the discrete set of equations in the X-FEM (Moës et al., 1999). The entries of the stiffness matrix are given by integrals with integrands that are discontinuous across the crack and/or are also weakly singular at the crack-tip. To accurately evaluate these contributions to the stiffness matrix, additional procedures are needed to perform the numerical integration.

First and foremost, since the crack is a line or surface discontinuity that intersects an enriched element, any numerical integration scheme must perform quadrature over the subdomains on either side of the crack. To this end, the simplest and most widely used approach is the partitioning of the finite element into subcells (triangles in $\mathbb{R}^2$ and tetrahedra in $\mathbb{R}^3$) for the purpose of numerical integration (Moës et al., 1999; Sukumar et al., 2000). In 2D, an enriched element is decomposed into a collection of triangles, with the crack conforming to the boundary edges of the triangles. It is worth pointing out that this procedure is *not equivalent to remeshing*, since no additional degrees of freedom accrue and in addition, there are no restrictions placed on the shape of these triangles. The partitioning is relatively easy to implement in 2D, but for multiple cracks with kinks in 3D, more sophisticated computational geometric algorithms are needed for an efficient and robust implementation. To avoid the need for partitioning the elements, algorithms have also been devised for polynomial-precision quadrature rules that integrate discontinuous functions on either side of the crack (Ventura, 2006; Holdych et al., 2008; Mousavi and Sukumar, 2010b; Ventura and Benvenuti, 2015); however, these approaches are still the subject of current research, and hence the partitioning procedure continues to be the preferred method-of-choice for numerical integration within the X-FEM.

Elements that contain the crack-tip in two dimensions or those that intersect the crack front in three dimensions require special treatment, since the crack-tip singularity lies within such elements. A higher-order tensor-product Gauss quadrature rule as adopted in Moës et al. (1999) and Sukumar et al. (2000) suffices for coarse-mesh accuracy. However, to demonstrate robustness of the method and to establish convergence for geometric enrichment (Laborde et al., 2005; Béchet et al., 2005), the singular (weakly) integrands must be accurately integrated to ensure optimal asymptotic rates of convergence. Use of Gauss quadrature limits the accuracy for such integrals, and hence in two dimensions an *almost-polar* transformation (Laborde et al., 2005), which is identical to the Duffy map (Duffy, 1982)), and a parabolic transformation (Béchet et al., 2005), were introduced. When the crack-tip is located within an element, the element is partitioned into triangles with the crack-tip located at a vertex of each triangle. Mousavi and Sukumar (2010a) generalized the Duffy transformation to integrate weakly singular integrands. In this approach, an affine transformation is first used to map each triangle to the standard triangle T_0 shown in Fig. 5. Then, the unit square (unit cube in 3D) is mapped to the standard

triangle (pyramid in 3D) via the transformation:

$$(u, v) \rightarrow (x, y) : x = u^{\beta}, \; y = xv = u^{\beta} v, \tag{5}$$

where $\beta \in \mathbb{Z}^{+}$. Consider integrating $f(\boldsymbol{x}) := g(\boldsymbol{x}) r^{-\alpha}$ over T_0, where $r = \sqrt{x^2 + y^2}$ and $g(x, y)$ is a bivariate polynomial. Then, on applying (5), the kernel becomes

$$K(u, v) := \frac{g(u^{\beta}, u^{\beta} v) |\boldsymbol{J}|}{r^{\alpha}} = \frac{g(u^{\beta}, u^{\beta} v) \beta u^{2\beta - 1 - \alpha\beta}}{\sqrt{1 + v^2}}, \tag{6}$$

where $|\boldsymbol{J}|$ is the Jacobian of the map in (5). The parameter β is selected so that the exponent of u in (6) is the smallest positive integer. For $\alpha = 1$, the $1/r$ singularity is eliminated with $\beta = 1$ (Duffy transformation), whereas for $1/\sqrt{r}$ ($\alpha = 1/2$), $\beta = 2$ is optimal. Since $1/r$ and $1/\sqrt{r}$ terms arise in the X-FEM for elastic fracture, this approach is accurate in two dimensions (Mousavi and Sukumar, 2010b; Minnebo, 2012; Cano and Moreno, 2015). Cano and Moreno (2015) provide a general prescription to obtain the map $\mathcal{D}_g$ that cancels the singularity. These integration schemes are also pertinent when other power singularities are present, for instance in applications such as as hydraulic fracture (Gordeliy and Peirce, 2015), crack impinging a bimaterial interface (Huang et al., 2003), and Poisson and elasticity problems with reentrant corners. For a crack front that represents a line singularity, Minnebo (2012) describes a comparison of existing approaches, and presents extensions of the Duffy and parabolic transformation schemes to integrate singular enrichment functions in 3D.

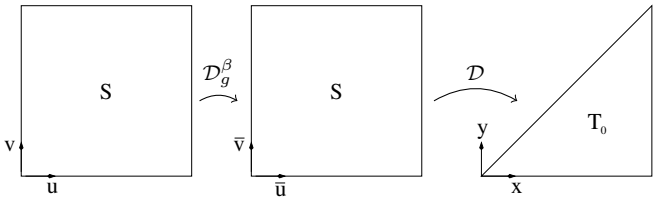

Fig. 5: Transformations from the unit square to the standard triangle. The Duffy transformation $\mathcal{D} : S \rightarrow T_0$ maps the unit square to the standard triangle. This is followed by a power transformation $\mathcal{D}_g^{\beta} : S \rightarrow S$ that maps the square onto itself. The composite map from $\boldsymbol{u} \rightarrow \boldsymbol{x}$ is: $x = u^{\beta}$, $y = u^{\beta} v$, where $\beta \in \mathbb{Z}^{+}$ (Mousavi and Sukumar, 2010a).

5 Conditioning of the linear system of equations

Conditioning issues may arise with the X-FEM, which come in two types. The first is related to the crack-tip enrichment, which was first observed in Laborde et al. (2005) and Béchet et al. (2005). Ill-conditioning in the X-FEM stems from the fact that on a given support of a nodal finite element basis function, the enriched basis functions may be nearly linearly dependent among themselves and/or with the finite element basis functions. We note in passing that instead of forming the partition-of-unity functions from the finite element shape functions, use of *flat-top* functions (Griebel and Schweitzer, 2000) ensures linearly independent basis functions and algorithms are available that mitigate ill-conditioning in the particle partition-of-unity method (Schweitzer, 2011). The crack-tip enrichments given in (4b) introduce 8 (12) additional degrees of freedom per node in 2D (3D). Globally, these enrichment functions are linearly independent. However, on an element-level the basis functions ($\{N_i F_{\alpha}\}$) that are associated with these enrichments can be linearly dependent, which was demonstrated in Laborde et al. (2005). With just topological enrichment, the ill-conditioning is not severe; however, it is exacerbated with geometric enrichment. This is due to two reasons: enriching many nodes within a fixed radius of the crack-tip can introduce low-energy modes; and away from the crack-tip, $\sqrt{r}$ resembles a polynomial that introduces near linear-dependencies between the enriched and FE basis functions. Fortunately, remedies exist. The one proposed in Laborde et al. (2005) is to reduce the number of enriched degrees of freedom by tying them together, leading to enrichment functions with larger support. This approach, however, compromises accuracy.

Another remedy is to enrich each component of the displacement field using the vectorial enrichment strategy discussed in Sect. 3.3. The impact of vectorial enrichment on conditioning was examined by Chevaugeon et al. (2013). Vectorial enrichment improves conditioning in large part because of the reduction in enriched degrees of freedom — a factor of four at each node in 3D.

Yet another way to improve conditioning is to design an ad hoc preconditioner (Béchet et al., 2005). The preconditioner is devised by considering all approximations functions related to a support and orthogonalizing them with respect to the bilinear form, i.e., block-preconditioning, with each block gathering all the degrees of freedom for a particular node.

The generalized Heaviside (discontinuous) enrichment can be the cause for the second type of ill-conditioning. Indeed, if the support of a basis function is cut by a crack that is very close to its boundary, the standard FE basis function and the enriched basis function will be nearly linearly-dependent. This issue may also arise if several cracks cross the support of a basis function, partitioning the support of the basis function into two pieces with

one volume significantly smaller than the other (Siavelis et al., 2013). Again, the specific X-FEM preconditioner designed in Béchet et al. (2005) is found to be efficient.

Very recently, a new design of the enrichment functions has been proposed to mitigate ill-conditioning in partition-of-unity finite element methods. It is coined SGFEM (stabilized generalized finite element method) (Babuška and Banerjee, 2012). The key idea is to remove from the enrichment function its piecewise linear continuous interpolant. The strategy is very efficient in terms of reducing the condition number and an error reduction is also observed. Indeed, the SGFEM does not give the same solution as the GFEM due to the elements that are located on the boundary of the enrichment region. On these elements, the new enrichment strategy appears to be more efficient. For a planar three-dimensional edge-crack problem with vectorial enrichment functions, Gupta et al. (2015) showed that the SGFEM improves accuracy and reduces the condition number vis-à-vis GFEM for topological as well as geometric enrichment strategies.

6 Implicit representation of cracks in three dimensions

In the X-FEM, cracks can be arbitrarily placed within a finite element mesh. Since cracks are modeled independent of the underlying FE mesh, their geometry needs to be stored in some other manner. To this end, one approach is to explicitly provide the crack geometry as a set of segments or parametric curves in two dimensions, and as a set of triangles (nonplanar surface) in three dimensions. Initial papers on the X-FEM did use this explicit representation. A major drawback to this approach is that it requires a completely separate infrastructure to represent the crack, beyond what the background finite element mesh can provide. Furthermore, while a great deal of progress has been made using explicit representations of crack geometries to simulate crack growth in three dimensions, the approach remains non-trivial for industrial-grade problems. We point the reader to Garzon et al. (2014) for insight into the state-of-the-art and remaining challenges. Considerations such as these have motivated the development and pursuit of alternative methods for representing crack geometries.

Level set and fast marching methods (Sethian, 1999) are numerical techniques for capturing moving interfaces. They provide an implicit way to store boundaries and to evolve them under known prescribed velocities on the boundaries. The boundary is represented as the zero level contour of a signed distance function that is associated with it. The signed distance function may be discretized by nodal values of a standard finite element field, and hence geometrical features are transformed into finite element fields.

For closed surfaces of codimension 1 in $\mathbb{R}^d$, the level set representation and implementation is straightforward. However, modeling cracks poses significant challenges, since a crack does not decompose a domain into two disjoint parts (except when the domain is fully cut). Hence, two level sets are needed to locate a crack: a normal level set function $\phi_n(\boldsymbol{x})$ and a tangential level set function $\phi_t(\boldsymbol{x})$. For representing 2D cracks, the use of level sets with the X-FEM was conceived in Stolarska et al. (2001), and the extension to 3D was presented in Moës et al. (2002) and Gravouil et al. (2002). The sign of the function $\phi_n(\boldsymbol{x})$ indicates if a point $\boldsymbol{x}$ is above or below the crack, and the function $\phi_t(\boldsymbol{x})$ provides the distance to the crack front. On combining the two, the crack discontinuity and the crack front of the discontinuity are represented by the sets

$$\Gamma_c = \{\boldsymbol{x} : \phi_n(\boldsymbol{x}) = 0 \text{ and } \phi_t(\boldsymbol{x}) < 0\}, \tag{7a}$$

$$\Lambda_c = \{\boldsymbol{x} : \phi_n(\boldsymbol{x}) = 0 \text{ and } \phi_t(\boldsymbol{x}) = 0\}. \tag{7b}$$

Figures 6a and 6b illustrate ϕ_n and ϕ_t in 2D and 3D, respectively.

In addition to providing the location of the crack, the use of these two level set functions offer additional advantages in extended finite element computations. First, on using $\phi_n(\boldsymbol{x})$ and $\phi_t(\boldsymbol{x})$, the local crack-tip coordinates (r, θ) (see Fig. 4) that are needed for evaluating enrichment functions are readily computed:

$$r = \sqrt{\phi_n^2 + \phi_t^2}, \quad \theta = \tan^{-1}\left(\frac{\phi_n}{\phi_t}\right). \tag{8}$$

Secondly, for even planar cracks (penny or elliptical in shape) within X-FEM or those meshed within FEM, knowing the associated level set fields is beneficial to express the auxiliary fields that arise in the domain form of the contour interaction integrals (see Sect. 7).

7 Extraction of stress intensity factors and crack growth simulations

The notion of stress intensity factors (SIFs), which is central to linear elastic fracture mechanics, appear in Williams's expansion of the stress field in the vicinity of the crack-tip. The three (constant) stress intensity factors K_I, K_{II} and K_{III} that correspond to the opening mode, in-plane shear mode, and out-of-plane shear mode, respectively, are sufficient to define the so-called K-dominant field. When small-scale yielding conditions

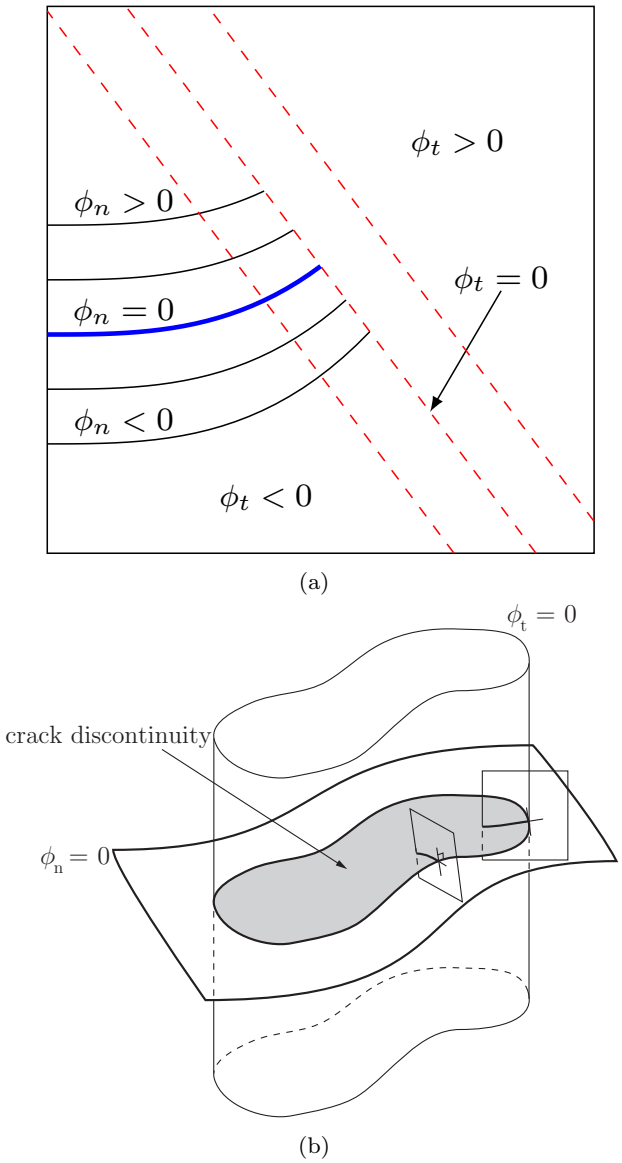

Fig. 6: Level set representation of a crack. Signed distance functions ϕ_n and ϕ_t to represent the crack interior and the crack tip/front, respectively. The functions are illustrated for 2D in (a) and for 3D in (b).

hold, the elastic K-field governs fracture and failure of the material. Irwin showed that the energy release rate (crack driving force) is related to the stress intensity factors. Stress intensity factors are used to both ascertain whether or not cracks will grow under given loading conditions, and also to determine the direction of crack propagation under mixed-mode loading conditions.

For stress intensity factor computations with finite elements or extended finite elements, the use of crack-tip flux integrals leads to better accuracy than displacement or stress extrapolation techniques. Domain forms of the contour J-integral and associated contour interaction integrals remain the most popular method for extracting SIFs from finite-element calculations (Yau et al., 1980; Li et al., 1985; Shih et al., 1986; Moran and Shih, 1987; Nakamura and Parks, 1989; Gosz and Moran, 2002). In the interaction integral method, the two-dimensional plane strain auxiliary fields are introduced and superposed on the actual fields that arise from the solution of the boundary-value problem. By judicious choice of the auxiliary fields, the contour interaction integral can be directly related to the mixed-mode stress intensity factors.

Interaction integral methods were employed in two-dimensional analysis with the X-FEM (Belytschko and Black, 1999; Moës et al., 1999). The domain representation of the interaction integral converts a contour integral around the crack-tip into an area integral over the region enclosed by the contour. Let this domain of integration be denoted by Ω_k^h. In two dimensions, the process is completed in three basic steps. First, one identifies all elements having a node within a specified radius $r_k := \alpha h_e$ of the crack-tip, where α is a scalar multiple and h_e is the crack-tip mesh size. This set of elements defines Ω_k^h. Then, a scalar-valued weight function, typically designated as $q(\boldsymbol{x})$, is constructed using the nodal shape functions of these domain elements. A common procedure is to use a *plateau* function for $q(\boldsymbol{x})$, which assumes a value of unity everywhere except near the boundary of the domain where it vanishes. Finally, contributions to the interaction integral, which involve field quantities and their gradient, are assembled by looping over these domain elements.

For planar cracks in three dimensions, the domain form of the J-integral is used (Sukumar et al., 2000), whereas for nonplanar cracks in three dimensions, the interaction integral method of Gosz and Moran (2002) is used to extract the SIFs in extended finite element computations (Moës et al., 2002; Sukumar et al., 2008). In three dimensions, the process is not as straightforward as in two dimensions, since the collections of elements that represent suitable domains for SIF extraction along the crack front are not so easily identifiable. An approach that was introduced in Sukumar et al. (2000) is to construct a completely independent group of hexahedral cells near a point on the crack front where SIFs are desired. Domain integrals are then assembled by looping over newly-created quadrature points in these cells. At each quadrature point in a cell, it is necessary to locate the position of the point in the original mesh and then extract the needed quantities such as the strain energy density. We note that these fields are discontinuous across element boundaries, and as such there is error

associated with the quadrature in these cells. SIFs obtained with this approach tend to exhibit small oscillations, as shown in Sukumar et al. (2000). One means to effectively smooth oscillations for SIFs along the crack front is to adopt a modal decomposition, such as that proposed by Galenne et al. (2007) for dynamic loading. While this technique was originally proposed for cracks that are meshed, it can be applied to embedded crack surfaces as in the X-FEM.

Under fatigue-type crack growth conditions, knowing the stress intensity factor distribution along the crack front for the maximum and minimum load in each cycle, the crack extent is computed from the Paris law for a given number of cycles. The crack growth direction is determined using the maximum hoop stress criterion (Erdogan and Sih, 1963). For two-dimensional cracks that are represented by piecewise linear segments, the exact geometry is available, and hence its extension during crack growth is simple. In three dimensions, the use of level set functions ϕ_n and ϕ_t is attractive to represent cracks during crack propagation simulations. On knowing the magnitude and orientation of crack growth, both ϕ_n and ϕ_t are updated using the level set method (Gravouil et al., 2002).

For monotonically advancing interfaces such as crack fronts, the fast marching method (FMM) (Sethian, 1999) has certain advantages over the level set method — FMM is a single-pass algorithm with no time-step restriction, which is unlike the level set method that is limited by a critical time-step to ensure stability. The FMM was first adopted for crack propagation simulations of planar cracks in Sukumar et al. (2003) and subsequently extended for nonplanar cracks in Sukumar et al. (2008). Duflot (2007) has presented an overview of various algorithms for the level set description for three-dimensional cracks. Since these initial papers, with an eye on robustness and speed, improvements have been proposed — use of a narrow band FMM by Shi et al. (2010) and use of alternative level set update equations by Colombo and Massin (2010).

8 Extensions beyond quasistatic elastic fracture

The preceding sections have focused on the modeling of cracks using the X-FEM within the purview of quasistatic linear elastic fracture mechanics. Of course, fracture phenomena is in general much richer and diverse, and the extended finite element method has been brought to bear on more complicated fracture problems in linear and nonlinear failure mechanics. Herein, we touch upon some of the more important and noteworthy developments along these lines, including cohesive models of fracture, dynamic fracture, and inelastic fracture governed by finite deformation kinematics and incompressible material behavior. We also discuss important advances concerning the development of models that enable transitions from damage to discrete fractures.

8.1 Cohesive models, dynamic fracture and nonlinear fracture

Cohesive models are one of the more prominent means to treat fracture and failure. They are characterized by an interfacial constitutive law (often nonlinear) relating tractions and displacements on crack faces. With cohesive models and the X-FEM, a key question concerns identifying the crack geometry and the extent of the cohesive region during the progression of the simulation. This aspect is addressed in depth in Moës et al. (2002). Another question concerns the stability of the formulation as the effective stiffness of the interface increases, an issue first raised by Ji and Dolbow (2004). This aspect has been addressed in part through both the development of stable (Ferté et al., 2014) and stabilized (Annavarapu et al., 2014) formulations for treating interfacial constitutive laws with the X-FEM. Mergheim et al. (2005) and Mergheim et al. (2007) have adopted the approach of Hansbo and Hansbo (2004) to simulate propagating cohesive cracks in quasi-brittle materials using small-strain and finite-strain kinematics, respectively.

While cohesive zone models are relatively straightforward in their implementation, dynamic fracture is not. Indeed, dynamic fracture has raised specific issues related to the X-FEM, including the need for appropriate mass lumping strategies and stable time integrators with near-tip enrichment (Menouillard et al., 2008). Schweitzer (2013) has proposed a variational mass lumping scheme for partition of unity methods, which holds promise for dynamic fracture. Robust time integration schemes remain an open issue, in the sense that the use of an explicit scheme precludes removing near-tip enrichment from nodes as a crack propagates. Conditional stability can only be guaranteed if the number of near-tip enriched degrees of freedom monotonically increases with time (Réthoré et al., 2005).

Up to this point, we have confined our attention to fracture problems in which the bulk material response is linearly elastic. The basic ideas of the X-FEM have also been adapted for other bulk material models, to varying degrees. For example, it is trivial to extend the concept of Heaviside enrichment to finite strains and nonlinear elasticity, as shown in Wells and Sluys (2001). However,

beyond linear elasticity, identifying near-tip enrichment functions that are sufficiently accurate to recover optimal rates of convergence becomes much more challenging (Legrain et al., 2005). Examples of recent attempts to identify suitable near-tip enrichment functions can be found in Elguedj et al. (2006) for plasticity and in Karoui et al. (2014) for compressible hyperelasticity.

With nearly-incompressible material response, the standard approach with finite elements is to employ mixed formulations (or their selective reduced-integration equivalents) that are stable. The first attempt at this with the X-FEM adopted an enhanced assumed strain formulation, and introduced the concept of a discontinuous version of the patch test (Dolbow and Devan, 2004). More generally, not all element formulations remain stable once Heaviside and/or near-tip enrichment is introduced. We point the reader to the work of Legrain et al. (2008) for an exposé on this topic.

8.2 Connecting damage and discrete fractures

We have emphasized that the X-FEM is, first and foremost, an *enabling technology*. It provides a means to introduce a discontinuity inside an element, as well as a network of discontinuities inside a mesh. It also provides a way to enhance finite element approximation functions beyond the standard piecewise-polynomial functions, such that near-tip singularities can be captured on relatively coarse meshes. It bears emphasis that such capabilities are not a replacement for the physics of fracture. In order to be robust, fracture simulations employing the X-FEM need to be based on sound theoretical underpinnings.

Robustness has proven to be elusive for complex three-dimensional crack growth simulations, where for example there is an interest in representing many crack surfaces that nucleate, interact, and merge. Several researchers have attempted to use relatively simple physical laws to nucleate and grow multiple crack surfaces in three dimensions, with varying degrees of success (Molino et al., 2004). While such approaches can undoubtedly enable fragmentation simulations, spatial convergence in various output quantities of interest has yet to be demonstrated. On occasion, failures in this arena have been attributed to the limitations of the X-FEM itself, but we contend that in fact the issue is a reliance on physical models that are unsound, combined with algorithms that employ heuristics.

We believe that a sound approach to treat this class of problems is to view the X-FEM as a means to transition from continuum damage models to discrete fracture surfaces. Early studies along these lines were performed by Simone et al. (2003) who modeled the transition from nonlocal damage to discrete cracks, and by Comi et al. (2007) who used enrichment functions in the X-FEM to facilitate the transition from a damage model to a cohesive zone model. We also mention the contribution of Seabra et al. (2012) who placed discontinuity surfaces in plastic zones for ductile failure, as well as the recent work of Tamayo-Mas and Rodriguez-Ferran (2015), who placed them in damage zones for quasi-brittle failure. Continuum damage models raise interesting theoretical questions when the capabilities of the X-FEM are considered. When a standard damage model is employed with finite elements, at some point damage accumulates to such a degree that some elements are completely degraded. These regions introduce a number of challenges, such as significant mesh distortion and poor conditioning. A crude way to treat such elements is to simply remove them from the discretization. But this approach results in a loss of mass, and fracture surfaces that are jagged.

In principle, the X-FEM provides an elegant approach to introduce a failure surface as damage progresses. But where should distinct fracture surfaces be placed for a given damage model, and how quickly should they advance? Surfaces that advance too quickly end up failing material that has not fully degraded. Conversely, surfaces that do not advance at the appropriate rate result in the same issues that were mentioned above, where regions of completely degraded elements can persist.

The aforementioned questions are not as much related to the X-FEM as they are to theoretical issues pertaining to the transition from damage to fracture. The recently proposed Thick Level Set (TLS) method (Moës et al., 2011) is an attempt at addressing these questions. In the TLS, the damage variable is tied to a level set field, from which the contour of the crack ($d = 1$) can be extracted. Damage reaches unity at exactly the same rate as the crack advances. Once the crack geometry is identified, the extended finite element technology is introduced to capture displacement jumps. The TLS also remedies a technological challenge with level sets and fracture surfaces, in the sense that a single level set field can be used for all the cracks in the domain. The method has been used to simulate complex fracture problems in three dimensions, including crack nucleation, branching, and coalescence.

9 Conclusions and future outlook

In this paper, we have provided our perspective on the main developments of the X-FEM (and related methods) in computational fracture mechanics. As stated in the introduction, this is not a review paper, but rather a synthesis of our views on the main thrusts in the X-FEM. We have concentrated on the use of the X-FEM for the simplest, but yet most widely-used mechanical failure model — linear elastic fracture mechanics with a crack growth model that only requires knowing the stress intensity factors along the crack front.

The extended finite element method is an advance in *element technology* for modeling cracks and to conduct crack growth simulations without the need for the finite element mesh to conform to the crack geometry. For crack modeling, the framework of partition-of-unity enrichment is used to construct the displacement approximation: Heaviside enrichment is used for the crack interior and elastic near-tip asymptotic enrichment functions are used for the crack tips. For comparable number of degrees-of-freedom, use of the X-FEM with *topological enrichment* (crack tips) yields better accuracy than quarter-point finite elements; however, both approaches deliver a (suboptimal) convergence rate of 1/2 in the energy seminorm. With *geometric enrichment* for the crack tips, the accuracy in the X-FEM is further enhanced, and more significantly, the optimal convergence rate of 1 in the energy seminorm for first-order Lagrange finite elements is realized. The flexibility that the X-FEM affords renders it particularly attractive to conduct parametric linear elastic fracture studies for cracks that have varying size, shape and location in complex geometries.

Notwithstanding the many advances and enhancements of the X-FEM for linear and nonlinear fracture computations, there still remain many challenges and open issues that can form the subject for future research. Further theoretical and numerical developments in r-adaptivity and goal-oriented error estimation techniques can ensure that a user-specified level of accuracy for the stress intensity factors can be met in elastic fracture analyses. Since geometric enrichment deteriorates the conditioning of the stiffness matrix, efficient preconditioners and solvers for ill-conditioned linear system of equations are of interest. Devising efficient numerical integration techniques without the need to partition the finite elements can lead to simplifications in the implementation of the X-FEM for fracture problems, and also enhance the robustness of the method. Since the crack geometry is not described by the FE mesh, the extraction of stress intensity factors using the volume representation of the interaction integral for three-dimensional crack configurations is, both, error prone and computationally demanding. Alternative approaches to compute SIFs in extended finite element need to be explored that are accurate, reliable and computationally efficient.

Conducting three-dimensional crack growth simulations poses an additional set of challenges to capture the evolution of cracks using level set functions. Variants of the fast marching method to update the level set functions for crack propagation simulations appear to be a fruitful direction to pursue. For dynamic fracture, suitable enrichment strategies and mass lumping techniques, and stable time-integration schemes can pave the way towards accurate simulations, while simulating fragmentation with a transition from continuum damage to discrete cracks remains a challenge. Finally, as an enabling technology, the X-FEM should now be also viewed as a numerical tool that allows one to assess and validate existing theoretical models against experiments and, in case such tests fail, provides the impetus towards the development of more appropriate models.

Acknowledgements The authors are grateful to the late Professor Ted Belytschko, with whom they coauthored many of the initial contributions on the X-FEM. His research ideas and technical writing have influenced our thinking and has helped us to shape this article. We also thank Professors David Chopp and Brian Moran, who introduced us to level set methods. N.S. is grateful for the research support of the National Science Foundation through contract grant CMMI-1334783 to the University of California at Davis. J.E.D. is grateful to the support from Sandia National Laboratories and Idaho National Laboratory, to Duke University; N.M. gratefully acknowledges the support of the ERC advanced grant XLS no. 291102.

References

Annavarapu, C., M. Hautefeuille, and J. E. Dolbow (2014). A Nitsche stabilized finite element method for frictional sliding on embedded interfaces. Part I: single interface. *Computer Methods in Applied Mechanics and Engineering 268*, 417–436.

Areias, P. M. A. and T. Belytschko (2006). A comment on the article 'A finite element method for simulation of strong and weak discontinuities in solid mechanics' by A. Hansbo and P. Hansbo [Computer Methods in Applied Mechanics and Engineering 2004; 193:3523–3540]. *Computer Methods in Applied Mechanics and Engineering 195*, 1275–1276.

Babuška, I. and U. Banerjee (2012). Stable generalized finite element method (SGFEM). *Computer Methods in Applied Mechanics and Engineering 201*, 91–111.

Babuška, I. and J. M. Melenk (1997). The partition of unity method. *International Journal for Numerical Methods in Engineering 40*, 727–758.

Béchet, E., H. Minnebo, N. Moës, and B. Burgardt (2005). Improved implementation and robustness study of the X-FEM for stress analysis around cracks. *International Journal for Numerical Methods in Engineering 64*(8), 1033–1056.

Bellec, J. and J. E. Dolbow (2003). A note on enrichment functions for modeling crack nucleation. *Communications in Numerical Methods in Engineering 19*, 921–932.

Belytschko, T. and T. Black (1999). Elastic crack growth in finite elements with minimal remeshing. *International Journal for Numerical Methods in Engineering 45*(5), 601–620.

Belytschko, T., R. Gracie, and G. Ventura (2009). A review of extended/generalized finite element methods for materials modeling. *Modelling and Simulation in Materials Science and Engineering 17*(4), 043001.

Belytschko, T., Y. Krongauz, D. Organ, M. Fleming, and P. Krysl (1996). Meshless methods: An overview and recent developments. *Computer Methods in Applied Mechanics and Engineering 139*, 3–47.

Benthem, J. P. (1977). State of stress at the vertex of a quarter-infinite crack in a half space. *International Journal of Solids and Structures 13*, 479–492.

Benzley, S. E. (1974). Representation of singularities with isoparametric finite elements. *International Journal for Numerical Methods in Engineering 8*, 537–545.

Cano, A. and C. Moreno (2015). A new method for numerical integration of singular functions on the plane. *Numerical Algorithms 68*(3), 547–568.

Chessa, J., H. Wang, and T. Belytschko (2003). On the construction of blending elements for local partition of unity enriched finite elements. *International Journal for Numerical Methods in Engineering 57*, 1015–1038.

Chevaugeon, N., N. Moës, and H. Minnebo (2013). Improved crack tip enrichment functions and integration for crack modelling using the eXtended Finite Element Method. *International Journal for Multiscale Computational Engineering 11*(6), 597–631.

Colombo, D. and P. Massin (2010). Fast and robust level set update for 3-D non planar X-FEM crack propagation modelling. *Computer Methods in Applied Mechanics and Engineering 200*(25–28), 2160–2180.

Comi, C., S. Mariani, and U. Perego (2007). An extended FE strategy for transition from continuum damage to mode I cohesive crack propagation. *International Journal for Numerical and Analytical Methods in Geomechanics 31*, 213–238.

Daux, C., N. Moës, J. Dolbow, N. Sukumar, and T. Belytschko (2000). Arbitrary branched and intersecting cracks with the extended finite element method. *International Journal for Numerical Methods in Engineering 48*(12), 1741–1760.

Dolbow, J. E. and A. Devan (2004). Enrichment of enhanced assumed strain approximations for representing strong discontinuities: addressing volumetric incompressibility and the discontinuous patch test. *International Journal for Numerical Methods in Engineering 59*, 47–67.

Duarte, C. A. and D. J. Kim (2008). Analysis and applications of a generalized finite element method with global-local enrichment functions. *Computer Methods in Applied Mechanics and Engineering 197*, 487–504.

Duarte, C. A. M., I. Babuška, and J. T. Oden (2000). Generalized finite element methods for three dimensional structural mechanics problems. *Computers and Structures 77*(2), 215–232.

Duffy, M. G. (1982). Quadrature over a pyramid or cube of integrands with a singularity at a vertex. *SIAM Journal on Numerical Analysis 19*(6), 1260–1262.

Duflot, M. (2007). A study of the representation of cracks with level sets. *International Journal For Numerical Methods in Engineering 70*(11), 1261–1302.

Duflot, M. and S. Bordas (2008). A posteriori error estimation for extended finite elements by an extended global recovery. *International Journal for Numerical Methods in Engineering 76*(8), 1123–1138.

Elguedj, T., A. Gravouil, and A. Combescure (2006). Appropriate extended functions for X-FEM simulation of plastic fracture mechanics. *Computer Methods in Applied Mechanics and Engineering 195*(7-8), 501–515.

Erdogan, F. and G. C. Sih (1963). On the crack extension in plates under plane loading and transverse shear. *Journal of Basic Engineering 85*, 519–527.

Ferté, G., P. Massin, and N. Moës (2014). Interface problems with quadratic X-FEM: design of a stable multiplier space and error analysis. *International Journal for Numerical Methods in Engineering 100*(11), 834–870.

Fix, G., S. Gulati, and G. I. Wakoff (1973). On the use of singular functions with the finite element method. *Journal of Computational Physics 13*, 209–228.

Fleming, M., Y. A. Chu, B. Moran, and T. Belytschko (1997). Enriched element-free Galerkin methods for crack tip fields. *International Journal for Numerical Methods in Engineering 40*, 1483–1504.

Fries, T. P. and T. Belytschko (2010). The extended/generalized finite element method: An overview of the method and its applications. *International Journal for Numerical Methods in Engineer-*

ing 84(3), 253–304.

Galenne, E., S. Andrieux, and L. Ratier (2007). A modal approach to linear fracture mechanics for dynamic loading at low frequency. *Journal of Sound and Vibration 299*(1–2), 283–297.

Garzon, J., P. O'Hara, C. A. Duarte, and W. G. Buttlar (2014). Improvements of explicit crack surface representation and update within the generalized finite element method with application to three-dimensional crack coalescence. *International Journal for Numerical Methods in Engineering 97*(4), 231–273.

González-Albuixech, V. F., E. Giner, and J. E. Tarancón (2015). Modeling of the free border singularity in 3D cracks using XFEM and spherical harmonics. *Revisita Internacional de Metodos Numericos para Calculo Y Diseno en Ingenieria 31*, 50–54.

Gordeliy, E. and A. Peirce (2015). Enrichment strategies and convergence properties of the XFEM for hydraulic fracture problems. *Computer Methods in Applied Mechanics and Engineering 283*, 474–502.

Gosz, M. and B. Moran (2002). An interaction energy integral method for computation of mixed-mode stress intensity factors along non-planar crack fronts in three dimensions. *Engineering Fracture Mechanics 69*(3), 299–319.

Gravouil, A., N. Moës, and T. Belytschko (2002). Non-planar 3D crack growth by the extended finite element and level sets—Part II: Level set update. *International Journal for Numerical Methods in Engineering 53*(11), 2569–2586.

Griebel, M. and M. A. Schweitzer (2000). A particle-partition of unity method for the solution of elliptic, parabolic and hyperbolic PDEs. *SIAM Journal on Scientific Computing 22*(3), 853–890.

Gupta, V., C. A. Duarte, I. Babuška, and U. Banerjee (2015). Stable GFEM (SGFEM): Improved conditioning and accuracy of GFEM/XFEM for three-dimensional fracture mechanics. *Computer Methods in Applied Mechanics and Engineering 289*, 355–386.

Hansbo, A. and P. Hansbo (2004). A finite element method for the simulation of strong and weak discontinuities in solid mechanics. *Computer Methods in Applied Mechanics and Engineering 193*(33–35), 3523–3540.

Holdych, D. J., D. R. Noble, and R. B. Secor (2008). Quadrature rules for triangular and tetrahedral elements with generalized functions. *International Journal for Numerical Methods in Engineering 73*(9), 1310–1327.

Huang, R., J.-H. Prévost, Z. Y. Huang, and Z. Suo (2003). Channel-cracking of thin films with the extended finite element method. *Engineering Fracture Mechanics 70*, 2513–2526.

Ji, H. and J. E. Dolbow (2004). On strategies for enforcing interfacial constraints and evaluating jump conditions with the extended finite element method. *International Journal for Numerical Methods in Engineering 61*, 2508–2535.

Jirásek, M. (2000). Comparative study on finite elements with embedded discontinuities. *Computer Methods in Applied Mechanics and Engineering 188*(1), 307–330.

Jirásek, M. and T. Belytschko (2002). Computational resolution of strong discontinuities. In H. A. Wang, F. G. Rammerstorfer, and J. Eberhardsteiner (Eds.), *Proceedings of Fifth World Congress on Computational Mechanics, WCCM V, Vienna University of Technology, Austria*.

Karoui, A., K. Mansouri, Y. Renard, and M. Arfaoui (2014). The eXtended finite element method for cracked hyperelastic materials: A convergence study. *International Journal for Numerical Methods in Engineering 100*(3), 222–242.

Laborde, P., J. Pommier, Y. Renard, and M. Salaün (2005). High-order extended finite element method for cracked domains. *International Journal for Numerical Methods in Engineering 64*(8), 354–381.

Legrain, G., N. Moës, and A. Huerta (2008). Stability of incompressible formulations enriched with X-FEM. *Computer Methods in Applied Mechanics and Engineering 197*, 1835–1849.

Legrain, G., N. Moës, and E. Verron (2005). Stress analysis around crack tips in finite strain problems using the eXtended finite element method. *International Journal for Numerical Methods in Engineering 63*(2), 290–314.

Li, F. Z., C. F. Shih, and A. Needleman (1985). A comparison of methods for calculating energy release rates. *Engineering Fracture Mechanics 21*(2), 405–421.

Linder, C. and F. Armero (2007). Finite elements with embedded strong discontinuities for the modeling of failure in solids. *International Journal for Numerical Methods in Engineering 72*, 1391–1433.

Melenk, J. M. and I. Babuška (1996). The partition of unity finite element method: Basic theory and applications. *Computer Methods in Applied Mechanics and Engineering 139*, 289–314.

Menouillard, T., J. Réthoré, N. Moës, A. Combescure, and H. Bung (2008). Mass lumping strategies for X-FEM explicit dynamics: Application to crack propagation. *International Journal for Numerical Methods in Engineering 74*, 447–474.

Mergheim, J., E. Kuhl, and P. Steinmann (2005). A finite element method for the computational modelling of cohesive cracks. *International Journal for Numerical*

Methods in Engineering 63, 276–289.

Mergheim, J., E. Kuhl, and P. Steinmann (2007). Towards the algorithmic treatment of 3D strong discontinuities. *Communications in Numerical Methods in Engineering 23*, 97–108.

Minnebo, H. (2012). Three-dimensional integration strategies of singular functions introduced by the XFEM in the LEFM. *International Journal for Numerical Methods in Engineering 92*, 1117–1138.

Moës, N., M. Cloirec, P. Cartraud, and J.-F. Remacle (2003). A computational approach to handle complex microstructure geometries. *Computer Methods in Applied Mechanics and Engineering 192*, 3163–3177.

Moës, N., J. Dolbow, and T. Belytschko (1999). A finite element method for crack growth without remeshing. *International Journal for Numerical Methods in Engineering 46*(1), 131–150.

Moës, N., A. Gravouil, and T. Belytschko (2002). Non-planar 3D crack growth by the extended finite element and level sets—Part I: Mechanical model. *International Journal for Numerical Methods in Engineering 53*(11), 2549–2568.

Moës, N., C. Stolz, P.-E. Bernard, and N. Chevaugeon (2011). A level set based model for damage growth: The thick level set approach. *International Journal For Numerical Methods in Engineering 86*, 358–380.

Molino, N., Z. Bao, and R. Fedkiw (2004). A virtual node algorithm for changing mesh topology during simulation. *ACM Transactions on Graphics 23*, 285–392.

Moran, B. and C. F. Shih (1987). Crack tip and associated domain integrals from momentum and energy balance. *Engineering Fracture Mechanics 27*(6), 615–641.

Mousavi, S. E. and N. Sukumar (2010a). Generalized Duffy transformation for integrating vertex singularities. *Computational Mechanics 45*(2–3), 127–140.

Mousavi, S. E. and N. Sukumar (2010b). Generalized Gaussian quadrature rules for discontinuities and crack singularities in the extended finite element method. *Computer Methods in Applied Mechanics and Engineering 199*(49–52), 3237–3249.

Nakamura, T. and D. M. Parks (1989). Anti-symmetrical 3-D stress field near the crack front of a thin elastic plate. *International Journal of Solids and Structures 25*(12), 1411–1426.

Nicaise, S., Y. Renard, and E. Chahine (2011). Optimal convergence analysis for the extended finite element method. *International Journal for Numerical Methods in Engineering 86*, 528–548.

Pereira, J. P. A., D.-J. Kim, and C. A. Duarte (2011). A two-scale approach for the analysis of propagating three-dimensional fractures. *Computational Mechanics 49*(1), 99–121.

Réthoré, J., A. Gravouil, and A. Combescure (2005). An energy-conserving scheme for dynamic crack growth using the eXtended finite element method. *International Journal for Numerical Methods in Engineering 63*(5), 631–659.

Richardson, C., J. Hegemann, E. Sifakis, J. Hellrung, and J. M. Teran (2011). An xfem method for modeling geometrically elaborate crack propagation in brittle materials. *International Journal for Numerical Methods in Engineering 88*(10), 1042–1065.

Rodenas, J. J., O. A. González-Estrada, J. E. Tarancón, and F. J. Fuenmayor (2008). A recovery-type error estimator for the extended finite element method based on *singular + smooth* stress field splitting. *International Journal for Numerical Methods in Engineering 76*, 545–571.

Schweitzer, M. A. (2011). Stable enrichment and local preconditioning in the particle-partition of unity method. *Numerische Mathematik 118*, 137–170.

Schweitzer, M. A. (2013). Variational mass lumping in the partition of unity method. *SIAM Journal on Scientific Computing 35*(2), A1073–A1097.

Seabra, M. R. R., P. Šuštarič, J. M. A. Cesar de Sa, and T. Rodič (2012). Damage driven crack initiation and propagation in ductile metals using XFEM. *Computational Mechanics 52*(1), 161–179.

Sethian, J. A. (1999). *Level Set Methods and Fast Marching Methods: Evolving Interfaces in Computational Geometry, Fluid Mechanics, Computer Vision, and Materials Science*. Cambridge, U.K.: Cambridge University Press.

Shi, J., D. Chopp, J. Lua, N. Sukumar, and T. Belytschko (2010). Abaqus implementation of extended finite element method using a level set representation for three-dimensional fatigue crack growth and life predictions. *Engineering Fracture Mechanics 77*(14), 2840–2863.

Shih, C. F., B. Moran, and T. Nakamura (1986). Energy release rate along a three-dimensional crack front in a thermally stressed body. *International Journal of Fracture 30*, 79–102.

Siavelis, M., M. Guiton, P. Massin, and N. Moës (2013). Large sliding contact along branched discontinuities with X-FEM. *Computational Mechanics 52*, 201–219.

Simo, J. C., J. Oliver, and F. Armero (1993). An analysis of strong discontinuities induced by strain-softening in rate-independent inelastic solids. *Computational Mechanics 12*, 277–296.

Simone, A., C. A. Duarte, and E. Van der Giessen (2006). A generalized finite element method for polycrystals with discontinuous grain boundaries. *International*

Journal for Numerical Methods in Engineering 67, 1122–1145.

Simone, A., G. N. Wells, and L. J. Sluys (2003). From continuous to discontinuous failure in a gradient-enhanced continuum damage model. *Computer Methods in Applied Mechanics and Engineering 192*(41–42), 4581–4607.

Song, J.-H., P. M. A. Areias, and T. Belytschko (2006). A method for dynamic crack and shear band propagation with phantom nodes. *International Journal for Numerical Methods in Engineering 67*, 868–893.

Stolarska, M., D. L. Chopp, N. Moës, and T. Belytschko (2001). Modelling crack growth by level sets in the extended finite element method. *International Journal for Numerical Methods in Engineering 51*(8), 943–960.

Strang, G. and G. Fix (1973). *An Analysis of the Finite Element Method*. Englewood Cliffs, N.J.: Prentice-Hall.

Strouboulis, T., K. Copps, and I. Babuška (2001). The generalized finite element method. *Computer Methods in Applied Mechanics and Engineering 190*(32–33), 4081–4193.

Sukumar, N., D. L. Chopp, E. Béchet, and N. Moës (2008). Three-dimensional non-planar crack growth by a coupled extended finite element and fast marching method. *International Journal for Numerical Methods in Engineering 76*(5), 727–748.

Sukumar, N., D. L. Chopp, N. Moës, and T. Belytschko (2001). Modeling holes and inclusions by level sets in the extended finite-element method. *Computer Methods in Applied Mechanics and Engineering 190*(46–47), 6183–6200.

Sukumar, N., D. L. Chopp, and B. Moran (2003). Extended finite element method and fast marching method for three-dimensional fatigue crack propagation. *Engineering Fracture Mechanics 70*(1), 29–48.

Sukumar, N., N. Moës, B. Moran, and T. Belytschko (2000). Extended finite element method for three-dimensional crack modelling. *International Journal for Numerical Methods in Engineering 48*(11), 1549–1570.

Sukumar, N. and J.-H. Prévost (2003). Modeling quasi-static crack growth with the extended finite element method. Part I: Computer implementation. *International Journal of Solids and Structures 40*(26), 7513–7537.

Tamayo-Mas, E. and A. Rodriguez-Ferran (2015). A medial-axis-based model for propagating cracks in a regularised bulk. *International Journal For Numerical Methods in Engineering 101*, 489–520.

Ventura, G. (2006). On the elimination of quadrature subcells for discontinuous functions in the eXtended finite-element method. *International Journal for Numerical Methods in Engineering 66*, 761–795.

Ventura, G. and E. Benvenuti (2015). Equivalent polynomials for quadrature in Heaviside function enriched elements. *International Journal for Numerical Methods in Engineering 102*(3–4), 688–710.

Wells, G. N. and L. Sluys (2001). A new method for modelling cohesive cracks using finite elements. *International Journal For Numerical Methods in Engineering 50*(12), 2667–2682.

Yau, J. F., S. S. Wang, and H. T. Corten (1980). A mixed-mode crack analysis of isotropic solids using conservation laws of elasticity. *Journal of Applied Mechanics 47*, 335–341.

Zi, G. and T. Belytschko (2003). New crack-tip elements for XFEM and applications to cohesive cracks. *International Journal For Numerical Methods in Engineering 57*, 2221–2240.

[1] Final publication is available at Springer via `http://dx.doi.org/10.1007/s10704-015-0064-8`